NATIONAL RESEARCH COUNCIL OF CANADA

DIVISION OF BUILDING RESEARCH

VIBRATION AMPLITUDES IN THE INUVIK POWERHOUSE

by

G. Pernica, V.R. Parameswaran and G.H. Johnston

DBR Paper No. 1283
of the
Division of Building Research

Ottawa, May 1985

TABLE OF CONTENTS

	PAGE
ABSTRACT	1
INTRODUCTION	1
LAYOUT OF THE POWERHOUSE	2
TEST PROCEDURE	3
ANALYSIS OF RECORDS	5
RESULTS	5
Narrow Band Analysis	5
One-Third Octave Band Analysis	6
Generator	6
Generator cradle-pile system	6
Generator cradle	6
Piles supporting the generator cradle	7
Comparison of cradle and pile response	7
Western section of powerhouse	8
Floor	8
Piles supporting floor	8
Comparison of floor and pile response	8
Eastern section of powerhouse	9
Floor	9
Piles supporting floor	9
Comparison of floor and pile response	10
Freestanding (unloaded) pile	10
Ambient acceleration amplitudes: generator off	11
SUMMARY AND CONCLUSIONS	11
ACKNOWLEDGEMENTS	12
REFERENCES	12
TABLES	13
FIGURES	29

ABSTRACT

Vibration measurements in the main powerhouse at Inuvik, NWT, were taken to determine the amplitudes of vibration present in a structure supported on pile foundations in permafrost and subjected to large dynamic periodic forces. Accelerometers were placed on the support system for the main diesel generator and on the floor and pile foundation of the one-storey industrial building. One-third octave band RMS acceleration amplitudes produced by the generator, a 5.2 MW system, are presented. In comparison to ambient acceleration amplitudes (generator off), amplitudes produced by the generator were approximately 430 times larger on the structural system supporting the generator and five to ten times larger throughout the remainder of the powerhouse.

INTRODUCTION

Foundations supporting buildings in permafrost areas are subjected to static and a variety of dynamic loads. Static loads include the weight and contents of the building. Periodic dynamic loads result from vibrating machinery (e.g., turbines, power generators, compressors), moving dynamic loads from cranes, fork lift trucks, etc., and shock and transient dynamic loads from such sources as stamps, forges, pile drivers, heavy vehicles, nearby blasting operations and earthquakes.

Pile foundations in permafrost are usually designed for static loads only, because information is lacking on the behaviour of frozen soils under dynamic loads. The designer generally uses empirically derived parameters and accepted design practices, as there are no established or standardized design criteria or codes. Piles are designed to support the vertical static load of the superstructure without exceeding an allowable settlement during the anticipated service life of the structure. When end bearing is not possible, as in ice-rich soils, the bearing capacity of a pile is assessed from the adfreeze bond strength between the pile and the soil. This strength has been experimentally determined from short-term laboratory tests and a few long-term pile load tests in the field. Unfortunately, there is considerable uncertainty in this procedure, due to variabilities in the type, temperature and moisture (ice) content of the soils and the surface characteristics of wood, concrete and steel piles. Hence a large factor of safety is incorporated into the design. The importance of pile creep in ice-rich soils has been recognized. As a result, pile design in ice-rich soils is presently based on limiting creep deformation; in ice-poor soils it is based on allowable adfreeze strengths (Weaver and Morgenstern, 1981).

Although the effects of dynamic stresses on the life of a pile foundation are not taken directly into consideration, the large factor of safety in design appears to compensate for these effects. Studies have shown that the dynamic Young's modulus decreases with increasing strain amplitude in ice and frozen soils. However, field studies of the effects of dynamic loads on the rate of settlement of piles in frozen soils have yet to be undertaken.

Laboratory model studies are underway at the Division of Building Research (DBR), National Research Council Canada (NRCC) to obtain information on the behaviour of piles in frozen soils under various

conditions of load and soil temperature. Preliminary results of these investigations showed that under creep conditions, an alternating stress as small as 5% of the static stress increased the displacement rate of wood and concrete piles in frozen sand and soils at about -2.5°C by a factor of 2 to 4 (Parameswaran, 1981 and 1984). This means, based on limiting creep displacements, that the service life of a structure can be reduced to one-half of that anticipated. One way of maintaining the desired service life of a structure and avoiding premature foundation failure, is to reduce the allowable static stress at the pile/soil interface.

In order that field conditions could be simulated in the laboratory experiments on piles, a field investigation of vibrations within an actual structure supported on pile foundations in permafrost had to be conducted. With the permission of the Northern Canada Power Commission (NCPC), the authors investigated the vibrations in the newer (1970) of two powerhouses in Inuvik, Northwest Territories, which is located in the continuous permafrost zone. The newer powerhouse was selected because it contained the main diesel generator for the town. Extensive measurements were carried out on the concrete floor of the powerhouse and on the wood foundation piles. The results of these measurements are presented in this paper. Measurements to determine the dynamic properties of wood piles in permafrost were also conducted on freestanding (unloaded) piles at two sites in Inuvik. Results of these measurements will be presented in a separate paper.

Before measurements were taken at the powerhouse, the authors were informed by Northern Canada Power Commission staff that the main diesel generator in the powerhouse did not operate as smoothly as similar diesel generators located in other northern communities. Vibration measurements taken on the generator by NCPC staff using hand-held probes indicated that the vibrations on the generator were approaching the upper end of the manufacturer's satisfactory operating range. As the main diesel generator was the only generator operating during the measurement period, the amplitudes of vibration contained in this paper are probably larger than those normally found for comparable generators elsewhere.

LAYOUT OF THE POWERHOUSE

The newer powerhouse in Inuvik (Figs. 1 and 2) is located adjacent to the East Channel of the Mackenzie River Delta. The rectangular one-storey industrial building is approximately 55.8 m long and 22.1 m wide, with the longitudinal axis parallel to the river channel. The powerhouse is completely supported on wood piles (Fig. 3).

The building was constructed in three stages: the western section, which contains the main diesel generator, was completed in 1970; the eastern section, which contains a smaller diesel generator for periods of peak load, was completed in 1975; and a small addition to the western section that contains ancillary equipment for the main diesel generator was completed in 1972 (Fig. 4). There are seven floor construction joints in the powerhouse building; the first separates the eastern and western sections of the building; the second separates the small addition and the western section; the third and fourth isolate the two diesel generators from the powerhouse floor; the fifth isolates a floor area in the western section that contains mechanical equipment (pumps and boilers); the sixth isolates a floor area in

the addition; and the seventh isolates a floor area in the eastern section that will ultimately be used for a future boiler. The dimensions of the three sections of the powerhouse and the location of each of the five isolated floor areas in the powerhouse are shown in Fig. 4.

The superstructure of the powerhouse consists of portal steel frames at 7.3 m spacings. The exterior walls and cladding of the superstructure are constructed from sheets of corrugated steel. The floor of the powerhouse, excluding the five isolated floor areas, is a one-way reinforced concrete slab approximately 200 mm thick. The slab is supported every 2.4 m by 610 mm wide × 460 mm deep reinforced concrete beams. The beams in turn are supported every 2.4 to 3.4 m by cylindrical wood piles (either Mackenzie Valley spruce or Douglas fir) that are embedded at least 150 mm into the underside of the concrete beams. In the western section of the powerhouse, the piles were from 250 to 300 mm in diameter and were embedded a minimum of 4.6 m in permafrost. In the eastern section, the pile diameter was 200 to 250 mm and the minimum embedment length was 6.1 m. The pile layout for the powerhouse is shown in Fig. 4. Details of piles in the western addition were not available.

Prior to construction of the concrete floor slabs, a gravelly fill was placed on the original ground surface, which slopes downward from the north side of the powerhouse to the south (river) side. The ground surface on the south side is approximately 2.5 m lower than that on the north side (Fig. 5). Figure 6 shows a cross-section through the western section of the building prior to construction. The permafrost table shown in Fig. 6 slopes in a comparable manner from the north side of the powerhouse towards the river. At the time of the measurements (September 1980), hand probing indicated that the depth of thaw was about 2.6 m on the south side of the building.

The two diesel generators housed in the powerhouse are supported on cradle-pile systems that are isolated from the floor of the powerhouse. Each generator comprises a diesel engine, a flywheel and an alternator (Fig. 7). The main generator, which was operating during the measurement period, is powered by a KV 16 Mirrlees Blackstone diesel engine manufactured by Hawker-Siddley of England. The 16 cylinder four-stroke engine operates at 514 rpm and has a rated peak load capacity of 5.2 MW. The generator is mounted on a 12.19 × 4.55 × 1.15 m reinforced concrete cradle (Fig. 8). The generator and cradle, which weigh approximately 300 tonnes, are supported by 28 wood piles. The piles are approximately 300 mm in diameter and are embedded at least 150 mm into the concrete cradle and about 5.0 m into permafrost. The pile layout is shown in Fig. 4 and a cross-sectional view through the concrete cradle is given in Fig. 9.

No information is given in this paper on the smaller diesel generator, since it was not in operation during the measurement period and since no vibration measurements were taken on the unit or on its supporting cradle-pile system.

TEST PROCEDURE

Vibration amplitudes produced by the KV 16 diesel engine were recorded using accelerometers placed at 35 locations at the Inuvik powerhouse. The

locations at the powerhouse are divided into the following three groups: nine on the main diesel generator and its supporting structure; 11 in the western section; and 15 in the eastern section (Fig. 4). No measurements were taken on the superstructure of the powerhouse. In the eastern section, transducers placed on the piles were located directly below transducer locations on the floor slab and approximately 300 mm below the underside of the concrete beam. Locations on piles and floor slab were chosen in pairs in order to determine the relative motion between the concrete floor and the supporting pile. For the main generator and the western section of the powerhouse it was not possible to pair all pile and floor locations because most of these piles were not readily accessible.

Vibration measurements were also taken on a freestanding (unloaded) wooden pile situated approximately 2 m from the south side of the powerhouse (Fig. 4). The spruce pile was 230 mm in diameter and had an above-ground height of 330 mm. It was assumed to be about 7 m long, based on the 4 m permafrost embedment length specified in the original design drawings for adjacent piles. This pile was monitored in order to determine the amplitudes of vibration of a single pile at some distance from a sizeable source of excitation.

At each accelerometer location, measurements were taken in the vertical direction. Except for a few locations, horizontal (perpendicular to the engine crankshaft and parallel to the long axis of the powerhouse) and axial (parallel to the engine crankshaft and the short axis of the powerhouse) directions were also monitored (Fig. 4). On the main generator, Bruel and Kjaer (B & K) 4332 piezo-electric accelerometers were used. These transducers have a flat response from 2 to 15000 Hz and a maximum operating temperature of 260°C. The accelerometers were attached to the generator using magnetic bases at the three locations recommended by the manufacturer for monitoring the unit's performance. At all other locations in the powerhouse, Q-flex QA 1100 servo-accelerometers (Sundstrand Data Control) with a sensitivity of 5 V/g from 0 to 500 Hz were used. The Q-flex accelerometers were attached to the concrete cradle and floor slab of the powerhouse using two-sided tape and to the wood piles using aluminum frames screwed to the piles (Fig. 10). Two-sided tape secured the accelerometers to the aluminum frame.

The outputs from the B & K and Q-flex accelerometers were amplified and low-pass filtered at approximately 630 Hz using a 6 dB/octave filter before being recorded on two FM tape recorders; a seven-channel Store 7D Racal and a four-channel 7003 Bruel and Kjaer. Twenty-eight runs, each approximately 20 minutes long, were made to record the vibrations produced by the main diesel generator at the 36 locations at the powerhouse site. Three runs were also made with the main generator turned off in order to measure the ambient vibration amplitudes at the powerhouse. For each run, only nine accelerometer outputs were recorded, as two accelerometer outputs were duplicated on each tape recorder. For runs 1 to 18, the frequency bandwidth of the recorded signals on the Racal was only 0 to 315 Hz, as the recording speed was set at 15/16 ips (24 mm/sec). The remaining runs were recorded on the Racal at 1 7/8 ips (48 mm/sec), which extended the frequency bandwidth to 630 Hz (the same as the low-pass filter).

ANALYSIS OF RECORDS

The recorded accelerometer signals were analyzed on a General Radio one-third octave band real time analyzer. The analyzer produces RMS levels in dB for the 30 one-third octave bands from 12.5 Hz to 10 kHz. One-third octave levels for frequency bands below 12.5 Hz were obtained from the recorded data by using playback to record speed ratios of eight on the Racal tape recorder and ten on the B & K. Identical ratios for the two tape recorders were impossible to achieve because of differences in tape recorder design. The above speed ratios shifted the effective frequency range of the analyzer; 1.6 Hz to 1.25 kHz for data stored on the Racal and 1.25 Hz to 1 kHz for data on the B & K.

Tables 1 to 11 contain one-third octave band acceleration amplitudes in percent gravity beginning at 2.5 Hz. Amplitudes for band frequencies below 2.5 Hz were omitted, since the lower frequency limit for the B & K accelerometers was 2 Hz. One-third octave band acceleration amplitudes were obtained from RMS levels in dB by calibrating the real time analyzer with a known input signal.

A one-second integration time was selected for the analyzer. Integration times for recorded data were eight seconds on the Racal and ten seconds on the B & K. Approximately 100 time averages (100 RMS levels per band) were obtained for each accelerometer record. The RMS acceleration amplitudes given in Tables 1 to 11 for each one-third octave band are 90th percentile values, i.e., 90% of the RMS amplitudes for a band are less than or equal to the 90th percentile amplitude. The 90th percentile was arbitrarily chosen as an upper bound for reporting purposes. For most of the accelerometer records, however, there was less than a 10% difference between the 90th and 50th percentiles in each band (small standard deviations).

Accelerometer signals at the three locations on the main diesel generator were also analyzed on a narrow band spectrum analyzer (Fourier Transform) to obtain the frequency spectrum of the forcing function within the powerhouse.

RESULTS

Narrow Band Analysis

Figures 11 to 13 contain the frequency spectra in the vertical direction at the three locations on the generator. Similar spectral distributions and content were obtained at each of the generator locations in the two lateral directions. The frequency content of vibrations on the KV 16 engine and on the alternator differ. Those on the diesel engine (locations 1 and 11; Figs. 11 and 12) are similar and contain many significant spectral peaks at frequencies above 100 Hz, while the vibrations on the alternator (location 13; Fig. 13) are composed primarily of frequencies below 100 Hz. The spacing between peaks in generator spectra is 4.28 Hz, which corresponds to the firing frequency of each cylinder. However, there is no visible peak at 4.28 Hz in any of the frequency spectra. The first noticeable peak occurs at 8.56 Hz, which corresponds to the frequency of rotation of the crankshaft.

One-Third Octave Band Analysis

The results of the one-third octave band analysis on accelerometer signals, grouped by structural location within the powerhouse, are presented in Tables 1 to 11. For accelerometer positions that were recorded on more than one run (e.g., generator location 13, vertical direction) one run was arbitrarily selected for presentation of the one-third octave band results, as the various runs produced similar amplitudes in most bands (Fig. 14). In bands with noticeable differences, amplitudes were at or near the noise floor of the recording-analysis system.

Generator

Table 1 contains the broadband and one-third octave band RMS acceleration amplitudes measured at the three locations on the main diesel generator (Fig. 4). No measurements were taken in the axial direction at location 11, since the accelerometer could not be properly secured to the diesel engine in this direction.

The following general observations were obtained from the results: (1) one-third octave band amplitudes in each direction on the alternator were significantly larger in the mid-frequency range (16 to 63 Hz) than corresponding amplitudes on the KV 16 engine (Fig. 15); (2) minimum broadband amplitudes on the generator were obtained in the horizontal and axial directions at the south (free) end of the engine and in the vertical direction on the alternator (Fig. 16); and (3) broadband and one-third octave band amplitudes in the two lateral directions on the KV 16 engine were larger at the flywheel end than at the free end (Figs. 15 and 16).

Generator cradle-pile system

Generator cradle: Table 2 contains the broadband and one-third octave band RMS acceleration amplitudes recorded at the four corners of the rectangular concrete cradle supporting the generator (Fig. 4). No measurements were taken in the horizontal and axial directions at location 3 since at the time of the measurements it was felt that in these directions there would be very little difference in acceleration amplitudes between locations 3 and 4.

Broadband and most one-third octave band amplitudes at locations 1, 2 and 4 were maximum in the vertical direction and minimum in the horizontal direction. As the generator cradle-pile system resembles an inverted pendulum, the lateral motions, particularly the horizontal, might have been expected to be larger than the vertical, especially in one-third octave bands containing lateral natural frequencies. Since the exact opposite occurred in nearly every band, the generator cradle-pile system may be softer in the vertical direction than in the lateral directions for frequencies below 315 Hz or the forcing function produced by the generator may be more in tune with vertical responses than with lateral responses.

Amplitudes in all three coordinate directions were larger at the south end of the cradle, locations 1 and 2, than at the north end, locations 3 and 4 (Figs. 17 and 18). This difference might be primarily due to the dynamic eccentricity present in the generator cradle-pile system. Although the centre of mass and centre of stiffness for the concrete cradle are

coincidental (no eccentricity) at the geometric centre of the cradle, they are neither coincidental nor at the geometric centre for the cradle-pile system. The mass centre of the system is located in the southern portion of the cradle, as the KV 16 diesel engine is considerably more massive than the alternator. The stiffness centre, on the other hand, is situated in the northern portion, as the total length and height above the ground surface of the foundation piles supporting the cradle increases from the north to the south end (Fig. 8). As a result of this dynamic eccentricity, the cradle-pile system would have a tendency (for most dynamic loads) to rotate about the stiffness centre, producing larger amplitudes at the south end than at the north end of the cradle.

Amplitudes in the two lateral directions on the alternator motor (Fig. 16) were substantially larger than the corresponding amplitudes at the north end of the cradle (Fig. 18). This perhaps indicates a need for a stiffer supporting structure for the alternator motor, which is attached to the top of a concrete pedestal (Fig. 7).

Piles supporting the generator cradle: Results of measurements taken on two piles at the southern end of the cradle are given in Table 3.

Broadband and most one-third octave band amplitudes in each coordinate direction on pile 5 were slightly larger than corresponding amplitudes on pile 6 (Fig. 19). Pile 5 also recorded the maximum broadband and one-third octave band amplitudes in the two lateral directions at the powerhouse; 69% g broadband, 55% g at 315 Hz in the horizontal direction and 55% g broadband, 39% g at 400 Hz in the axial direction. For broadband and one-third octave bands below 31.5 Hz and above 125 Hz, maximum RMS amplitudes on piles 5 and 6 were obtained in the horizontal direction and minimum in the vertical direction (the opposite occured on the cradle). For the remaining bands (31.5 Hz to 125 Hz), the order was reversed; the vertical direction had the maximum and either the horizontal or axial direction, the minimum. This reversal may indicate the one-third octave band locations of cradle-pile natural frequencies; fundamental lateral modes below 31.5 Hz and the fundamental vertical mode between 31.5 Hz and 125 Hz.

Comparison of cradle and pile response: During several runs, locations on the cradle piles and on the cradle were monitored simultaneously. Figures 20 to 22 plot the one-third octave band spectra obtained during Runs 24 to 26 at pile location 5 and cradle location 2. The cradle location is almost directly above the pile.

Spectral results indicate that in the vertical and axial directions (Figs. 20 and 21), the cradle-pile system behaves as a cantilever with a large tip mass having the following dynamic characteristics; 1) for natural frequencies below 250 Hz, modal responses are larger at the top of the cradle than near the top of the piles; and 2) between 250 and 500 Hz, the modal response of one or more natural frequencies is primarily pile response.

In the horizontal direction, the system appears to behave in a similar way but with some restraint at or near the top of the cradle for natural frequencies below 63 Hz. The slightly larger pile amplitudes below 63 Hz (Fig. 22) suggest that the concrete cradle is restrained to some degree by the concrete floor slab of the western section of the powerhouse. The

original 13 mm construction joint separating the cradle-pile system from the floor system may have closed at one or more points along one of the north-south sides. The substantially larger pile amplitudes between 250 Hz and 500 Hz again indicate natural frequencies with modes containing primarily pile responses.

Western section of powerhouse

Floor: Broadband and one-third octave band RMS amplitudes at the seven locations that were monitored on the floor of the western section of the powerhouse (Fig. 4) are given in Table 4. In general, RMS amplitudes decreased with increasing distance from the generator. The maximum broadband and one-third octave band amplitudes in each direction usually occurred on the floor at the alternator end of the cradle (location 4 or 5) and the minimum at location 7, which was the farthest from the generator (Figs. 23 and 24). Except at location 7, the maximum broadband amplitude at each floor location occurred in the vertical direction (Fig. 24). Axial broadband amplitudes were minimal at locations on either side of the generator (locations 1 and 6) and horizontal amplitudes were minimal at locations directly in front of or directly behind the generator (locations 2, 3, 4 and 5).

Broadband and one-third octave band amplitudes on the floor beside the cradle varied with location. Locations 4 and 5 along the alternator end of the cradle registered larger amplitudes in all three directions than those at locations 1 and 6 situated midway along either side of the cradle. The largest differences between the two groups occurred in the vertical direction and the smallest in the horizontal.

Piles supporting floor: Results of the measurements on four piles supporting the western section of the powerhouse (Fig. 4) are given in Table 5. The three piles located on the south side of the powerhouse (piles 2, 3 and 7) have above ground heights of approximately 3 m. Pile 4, located on the opposite side of the powerhouse, has at most 0.5 m exposed above the surface of the ground.

The maximum broadband amplitudes in the three coordinate directions were obtained on pile 3, the pile closest to the cradle, and the minimum on pile 7, the pile farthest from the cradle (Fig. 25). Vertical broadband amplitudes exhibited the most consistent decrease with distance from the cradle. In the two lateral directions the decreases with distance were only apparent when amplitudes on pile 7 were compared with those on the other three piles.

Except for pile 4, the maximum broadband RMS amplitudes at each pile location were obtained in the horizontal direction and the minimum in the vertical. On pile 4 the maximum occurred in the axial direction and the minimum in the horizontal.

Comparison of floor and pile response: At three locations in the western section of the powerhouse (locations 2, 3 and 7), measurements were taken on the concrete floor slab and on the pile foundation directly below. In the horizontal and axial directions, one-third octave band amplitudes on the piles were larger than those on the floors for nearly all bands (Fig. 27). Below 31.5 Hz the differences, if any, were small; pile and

floor locations could be considered to have identical responses. Above 31.5 Hz, pile amplitudes were significantly larger than floor amplitudes. The order of magnitude difference above 160 Hz probably indicates higher modes, with mode shapes consisting primarily of pile responses.

In the vertical direction, neither the piles nor the floors had consistently larger amplitudes for one-third octave bands below 160 Hz, even though pile/floor or floor/pile ratios at each location were as large as three throughout this frequency range (Fig. 28). Above 160 Hz, the effect of probable modal frequencies, with mode shapes consisting primarily of pile response, was again evident as amplitudes on the piles were significantly larger than those on the floor.

Eastern section of powerhouse

Floor: Broadband and one-third octave band amplitudes at seven locations on the floor of the eastern section of the powerhouse are given in Table 6. Measurements at location 6 were omitted because of time constraints.

In general, broadband and one-third octave band amplitudes on the floor of the eastern section of the powerhouse decreased with increasing distance from the generator. Of the three directions, the vertical sustained the largest and most consistent decrease with distance and the horizontal the smallest and the least consistent decrease (Fig. 29). In the vertical direction, broadband amplitudes decreased monotonically from an average of 2.2% gravity at the two locations nearest the generator (locations 7 and 8) to 0.29% gravity at the two locations farthest from the generator (locations 1 and 2). In the axial direction minimum broadband amplitudes occurred in the centre of the eastern section of the powerhouse (locations 3 and 4) rather than at the eastern end (locations 1 and 2).

Except for location 8, broadband amplitudes on the eastern floor were less than 1% gravity. At location 8, which was the closest to the cradle, broadband amplitudes in the vertical, axial and horizontal directions were 3.5, 1.6 and 1.2% gravity, respectively. Location 7, which is only 1 m farther from the cradle, had broadband amplitudes which were less than half those at location 8. It appears that more energy is transmitted into the powerhouse floor (eastern and western sections) at the alternator end than at the free end of the generator.

Piles supporting floor: Broadband and one-third octave band amplitudes at the seven pile locations under the floor of the eastern section of the powerhouse are given in Table 7. At most of these pile locations, broadband amplitudes in the horizontal direction were the largest and those in the vertical direction the smallest.

Amplitudes on the piles generally decreased with increasing distance from the generator (Figs. 30 and 31). The decrease was quite similar to that exhibited by the floor amplitudes. In the vertical direction broadband amplitudes decreased monotonically with distance, from 0.97% gravity at location 7 to 0.27% gravity at location 1. In the axial direction, minimum broadband amplitudes occurred (as was the case for the floor) in the centre of the eastern section of the powerhouse (locations 3 and 4) rather than at the eastern end (locations 1 and 2).

The minimum broadband pile amplitudes measured at the powerhouse were obtained on piles in this section of the powerhouse. These were 0.27% gravity in the vertical direction on piles 1 and 2, 0.49% gravity in the horizontal direction on piles 1, 3 and 4, and 0.39% gravity in the axial direction on pile 4.

Comparison of floor and pile response: At six of the eight locations in the eastern section of the powerhouse, measurements were taken on the concrete floor slab and on the pile directly beneath the floor (Fig. 4). In the horizontal and axial directions, noticeable amplitude differences between the pile and the floor occurred at all locations for one-third octave band frequencies greater than 160 Hz. At some locations, such as 7, the differences began at band frequencies as low as 50 Hz (Fig. 32). Regardless of where the differences commenced, the pile response above this frequency was larger than the floor response and, similar to the other two monitored structure-pile systems at the powerhouse (i.e., cradle-pile system and western section of powerhouse), was indicative of lateral modes with mode shapes consisting primarily of pile response. On the other hand, one-third octave band floor and pile spectra in the vertical direction at each location were quite similar in shape and amplitude throughout most of the frequency bandwidth (0-315 Hz).

As a result of the spectral differences in the horizontal and axial directions, broadband amplitudes in the two lateral directions were generally larger on the piles than on the floor (Table 8). However, in the vertical direction similar spectral shapes produced broadband amplitudes on the floor that were slightly larger than pile amplitudes at all locations. Except for the horizontal direction at location 7, pile/floor broadband amplitude ratios in the two lateral directions and floor/pile amplitude ratios in the vertical direction were between 0.9 and 1.5. In the horizontal direction at location 7, the pile/floor amplitude ratio was 3.7.

Freestanding (unloaded) pile

Results of the measurements taken on the freestanding pile located on the south side of the powerhouse approximately 11 m from the generator cradle and 2 m from the nearest pile supporting the eastern section of the powerhouse (Fig. 4) are given in Table 9.

Broadband amplitudes on the freestanding pile were smaller than the minimum broadband pile amplitudes recorded at the powerhouse with the generator on (Table 10). In comparison to the nearest monitored pile under each of the three structure-pile systems investigated at the powerhouse, the broadband amplitudes on the freestanding pile were from 5 to 250 times smaller in the two lateral directions and from 5 to 125 times smaller in the vertical direction (Table 10). It is also evident from Table 10 that for the powerhouse the degree of structural isolation of a structure-pile system from a source of vibration (or the degree of connectivity to it) was more important in determining the amplitudes of pile vibration than was the distance of the pile from the source. Pile location 7 in the eastern section of the powerhouse, which was more structurally isolated (no direct structural links) from the generator than pile location 2 in the western section, had substantially smaller amplitudes even though pile 7 was closer to the generator. The same can be said for the freestanding pile when

compared to either pile location 1 or 4 in the eastern section of the powerhouse.

Ambient acceleration amplitudes: generator off

Vibration measurements at eight locations (nine accelerometers) were taken with the generator turned off in order to ascertain ambient acceleration amplitudes throughout the powerhouse. Unfortunately, not all the mechanical equipment ancillary to the generator could be turned off with the generator. Several pumps and compressors associated with cooling the KV 16 engine after shut-down, and located in the western section of the powerhouse at the south end of the generator, continued to operate during the short time interval that the generator was off. The ambient vibration measurements, therefore, contain the effects of this mechanical equipment.

Broadband and one-third octave band amplitudes for the nine ambient accelerometer records are given in Table 11. Of these, five were on the cradle-pile system supporting the generator, two on piles supporting the western section and two on piles supporting the eastern section of the powerhouse. Broadband amplitudes at all locations were quite low, between 0.062% and 0.83% gravity, with the lower amplitudes obtained primarily on the piles supporting the generator cradle.

Broadband amplitudes obtained at the same accelerometer locations with the generator operating are also given in Table 11. Average on/off amplitude ratios were 430 for piles under the generator cradle and 10 and 5 respectively for piles supporting the western and eastern sections of the powerhouse. Obviously, the generator produced sizeable vibration amplitudes within its supporting cradle-pile system. On the other hand, vibration amplitudes in the eastern section with no direct structural ties to the cradle-pile system and linked only to the western section of the powerhouse via the steel superstructure, were considerably less affected by the presence of the generator. The slightly larger increase in the vibration environment of the western section of the powerhouse appears to have been caused by direct contact of this section with the cradle-pile system rather than by ground transmission of the vibrations between the two systems.

SUMMARY AND CONCLUSIONS

(1) Acceleration measurements at various locations in the Inuvik powerhouse showed that the vibration environment at the powerhouse was considerably affected by the operation of the main diesel generator.

(2) The amplitude of the forced vibrations at a monitored location was dependent on the structural connectivity of that location to the generator-cradle system and its distance from that system. Decreasing the degree of connectivity or increasing the distance decreased the amplitude.

(3) Piles underwent comparable acceleration amplitudes in all three translational directions, indicating that lateral as well as axial vibrations should be considered in the design of piles in permafrost.

(4) Although no information is available concerning the performance of the pile foundations of the powerhouse, laboratory studies indicate that the dynamic stresses transmitted to the adfreezing interface between a pile and frozen soil could enhance the displacement rate of the pile in soil, and thereby shorten the service life of a structure based on a specified allowable settlement. A knowledge of the amplitudes and frequencies of vibrations likely to result from operation of large vibrating or rotating machinery is essential for the safe design of pile foundations in permafrost.

ACKNOWLEDGEMENTS

Before measurements were conducted at the Inuvik powerhouse, discussions were held at the Edmonton offices of the Northern Canada Power Commission with the late Mr. J. Long, General Manager, Mr. J.D. Allan, Assistant General Manager, Operations and Engineering, and Mr. D.I. McGuinness, Engineering Manager. The authors wish to thank these gentlemen for providing the necessary background information and technical drawings. At the Inuvik powerhouse, Mr. J.H. Greenwood, Area Superintendent, and Mr. D.H. Musselwhite, Assistant Superintendent, were most helpful in making the necessary arrangements for conducting the study. The assistance and cooperation received from all NCPC staff is gratefully acknowledged.

The authors would also like to thank Mr. J.C. Plunkett, Geotechnical Section, Division of Building Research, National Research Council Canada, for his invaluable technical assistance during the measurement program at the Inuvik powerhouse.

REFERENCES

(1) Weaver, J.S. and Morgenstern, N.R. (1981) "Pile Design in Permafrost." Canadian Geotechnical Journal, Vol. 18, No. 3, p. 357-370.

(2) Parameswaran, V.R. (1982) "Displacement of Piles Under Dynamic Loads in Frozen Soils." The Roger J.E. Brown Memorial Volume, Proceedings Fourth Canadian Permafrost Conference, Calgary, Alberta, March 2-6, 1981, p. 555-559.

(3) Parameswaran, V.R. (1984) "Effect of Dynamic Loads on Piles in Frozen Soils." Proceedings of the Third International Specialty Conference on Cold Regions Engineering, Edmonton, Alberta, April 1984, Vol. I, p. 41-52.

TABLE 1

One-Third Octave Band RMS Acceleration Amplitudes on the Generator, % Gravity, 90th Percentile

Generator Location	1			11		13		
Tape Recorder	B & K			RACAL		B & K		
Run No.	1	1	3	1	6	1	1	3
				Direction*				
Frequency	V	H	A	V	H	V	H	A
Broadband	31	11	8.7	30	26	20	23	29
2.5	0.23	0.058	0.058	0.41	0.92	0.13	0.26	0.26
3.15	0.20	0.058	0.073	0.41	0.92	0.13	0.21	0.21
4.0	0.20	0.26	0.32	0.41	0.92	0.12	0.21	0.23
5.0	0.20	0.12	0.13	0.36	0.73	0.12	0.21	0.23
6.3	0.46	0.41	0.091	0.41	0.82	0.37	0.47	0.47
8.0	0.81	0.23	0.20	0.82	1.0	0.37	0.66	0.33
10.0	0.32	0.10	0.12	0.58	0.82	0.15	0.29	0.23
12.5	0.46	0.41	0.36	0.58	0.92	0.33	0.42	0.74
16	0.81	0.18	0.26	0.58	1.2	0.93	1.2	2.3
20	0.51	0.51	0.41	1.0	1.2	0.66	3.3	4.2
25	1.6	0.65	0.26	1.6	1.8	3.3	6.6	15
31.5	1.2	1.3	0.32	1.8	4.6	4.2	7.4	5.2
40	1.2	1.0	0.58	1.6	4.6	4.7	15	4.2
50	1.6	0.91	0.46	3.2	3.3	7.4	10	4.2
63	2.6	1.8	1.0	4.1	6.5	12	4.7	6.6
80	3.2	1.6	0.81	4.6	5.2	9.3	4.2	15
100	4.6	2.0	1.3	5.1	5.8	2.9	3.3	13
125	3.6	1.8	1.3	6.5	5.2	4.2	4.2	10
160	5.8	2.3	1.8	6.5	7.3	4.2	4.7	5.2
200	10	2.3	2.9	10	12	2.1	2.1	1.7
250	9.1	1.6	2.9	20	12	1.9	1.5	1.7
315	12	2.9	3.2	20	13	1.2	1.2	2.3
400	20	6.5	5.1			2.3	1.0	2.9
500	9.1	5.1	3.2			1.5	1.0	1.3
630	9.1	2.3	2.3			1.9	1.2	0.93

*Measurements were not taken in the axial direction at location 11, since the accelerometer could not be properly secured to generator.

TABLE 2

One-Third Octave Band RMS Acceleration Amplitudes on the Concrete Cradle of the Generator, % Gravity, 90th Percentile

Generator Cradle Location	1			2			3	4		
Tape Recorder Run No.	RACAL 1	RACAL 6	RACAL 3	RACAL 1	RACAL 26	RACAL 25	RACAL 1	RACAL 1	RACAL 6	RACAL 3
Frequency	Direction* V	H	A	V	H	A	V	V	H	A
Broadband	30	7.6	12	30	18	20	17	11	4.2	8.6
2.5	0.039	0.022	0.019	0.039	0.044	0.039	0.039	0.039	0.022	0.019
3.15	0.039	0.022	0.019	0.039	0.039	0.039	0.039	0.039	0.022	0.019
4.0	0.055	0.043	0.11	0.039	0.069	0.087	0.039	0.039	0.022	0.069
5.0	0.039	0.027	0.069	0.039	0.044	0.062	0.039	0.039	0.022	0.043
6.3	0.049	0.027	0.043	0.055	0.039	0.039	0.039	0.039	0.022	0.027
8.0	0.77	0.35	0.55	0.98	0.49	0.44	0.22	0.31	0.22	0.11
10.0	0.39	0.15	0.31	0.49	0.22	0.22	0.11	0.16	0.097	0.087
12.5	0.28	0.15	0.14	0.39	0.11	0.39	0.077	0.077	0.11	0.17
16	0.78	0.39	0.39	0.35	0.20	0.77	0.44	0.35	0.11	0.35
20	0.62	0.69	0.55	0.62	0.55	0.98	1.4	1.2	0.22	0.35
25	2.5	1.2	2.2	1.4	1.4	3.9	3.5	2.2	0.35	0.49
31.5	4.9	0.69	0.97	7.8	1.5	14	4.4	2.5	1.2	1.1
40	4.4	1.7	1.1	4.9	3.1	2.7	6.2	3.1	1.7	0.87
50	4.4	1.9	1.5	6.9	2.7	1.7	8.7	6.9	1.2	1.5
63	6.9	1.9	2.7	12	3.9	4.9	7.7	4.9	1.4	3.1
80	12	1.9	4.3	12	4.4	5.5	6.9	3.5	1.1	2.7
100	19	2.4	6.1	19	6.2	6.2	4.9	3.9	1.2	4.3
125	11	1.7	3.9	9.8	5.5	3.5	3.9	2.7	1.9	3.1
160	8.7	1.9	5.5	6.2	4.4	5.5	1.9	1.5	1.1	3.5
200	8.7	3.1	4.3	6.2	7.7	3.5	2.2	0.77	0.69	2.4
250	3.9	2.2	3.5	7.7	6.9	3.5	3.5	0.77	0.97	2.7
315	2.5	3.5	2.7	6.9	6.9	2.7	1.4	0.77	1.7	3.1

*No measurements were taken in the horizontal and axial directions at location 3 since it was felt that the results would be similar to those obtained at location 4.

TABLE 3

One-Third Octave Band RMS Acceleration Amplitudes on Piles Supporting the Generator Cradle, % Gravity, 90th Percentile

Pile Location	5			6		
Tape Recorder	RACAL			RACAL		
Run No.	24	26	25	24	26	25
Frequency	Direction V	H	A	V	H	A
Broadband	22	69	55	18	44	19
2.5	0.039	0.098	0.069	0.044	0.098	0.035
3.15	0.039	0.098	0.069	0.039	0.087	0.035
4.0	0.039	0.25	0.17	0.069	0.098	0.087
5.0	0.039	0.15	0.11	0.044	0.069	0.055
6.3	0.039	0.078	0.069	0.039	0.069	0.035
8.0	0.69	0.62	0.15	0.55	0.49	0.49
10.0	0.31	0.28	0.11	0.25	0.22	0.22
12.5	0.25	0.39	0.25	0.16	0.31	0.22
16	0.27	0.44	0.55	0.55	0.39	0.25
20	0.44	0.87	0.78	0.49	0.69	0.55
25	0.97	1.5	0.49	1.5	1.5	1.4
31.5	4.9	2.5	1.2	2.7	2.5	1.7
40	2.7	2.2	0.98	2.2	1.7	1.5
50	4.4	2.8	1.4	2.5	2.5	1.9
63	6.2	4.9	2.0	3.9	3.9	2.5
80	6.2	3.1	2.5	4.9	2.2	2.2
100	8.7	2.8	4.9	6.2	1.4	4.9
125	3.9	1.5	2.5	2.7	1.1	2.2
160	1.9	1.7	2.2	1.2	0.98	1.9
200	1.9	4.4	3.1	2.2	3.1	1.9
250	2.2	6.9	6.9	1.9	3.9	2.7
315	12	55	35	3.9	14	5.5
400	8.7	25	39	14	35	11
500	3.9	14	17	6.9	15	9.8
630	1.4	1.7	2.2	3.1	3.9	6.2

TABLE 4

One-Third Octave Band RMS Acceleration Amplitudes
on the Floor of the Western Section of the Powerhouse,
% Gravity, 90th Percentile

Floor Location	1			2			3		
Tape Recorder	RACAL			RACAL			RACAL		
Run No.	14	18	15	14	18	15	14	18	15
				Direction					
Frequency	V	H	A	V	H	A	V	H	A
Broadband	3.9	2.2	1.1	1.2	0.76	0.96	3.0	1.4	2.0
2.5	0.0078	0.0039	0.0019	0.0039	0.0019	0.0019	0.0078	0.0039	0.0078
3.15	0.0078	0.0039	0.0024	0.0039	0.0019	0.0024	0.0078	0.0039	0.0078
4.0	0.0078	0.012	0.035	0.0039	0.017	0.039	0.0078	0.015	0.039
5.0	0.0078	0.0098	0.027	0.0039	0.012	0.031	0.0078	0.011	0.031
6.3	0.0078	0.0087	0.027	0.0078	0.0087	0.035	0.0078	0.0098	0.035
8.0	0.011	0.028	0.14	0.11	0.097	0.19	0.078	0.098	0.22
10.0	0.0087	0.031	0.077	0.087	0.043	0.11	0.044	0.049	0.12
12.5	0.0087	0.078	0.055	0.049	0.024	0.055	0.025	0.035	0.055
16	0.039	0.39	0.14	0.098	0.061	0.15	0.069	0.044	0.17
20	0.055	0.44	0.11	0.14	0.087	0.14	0.098	0.087	0.14
25	0.14	0.31	0.097	0.20	0.087	0.31	0.12	0.078	0.28
31.5	0.49	0.78	0.22	0.44	0.35	0.43	0.78	0.39	0.25
40	1.5	0.78	0.35	0.15	0.061	0.15	0.44	0.35	0.20
50	2.5	0.55	0.24	0.39	0.077	0.22	0.87	0.55	0.25
63	1.2	0.69	0.35	0.44	0.12	0.19	0.98	0.35	0.31
80	1.5	1.1	0.39	0.49	0.22	0.19	1.5	0.39	0.28
100	1.1	0.98	0.55	0.49	0.43	0.35	0.98	0.77	0.31
125	0.69	0.44	0.43	0.49	0.27	0.22	0.87	0.55	0.69
160	0.35	0.31	0.27	0.22	0.14	0.24	0.78	0.27	0.35
200	0.28	0.31	0.22	0.35	0.22	0.35	0.69	0.35	0.62
250	0.20	0.22	0.22	0.27	0.17	0.35	0.69	0.31	1.4
315	0.28	0.19	0.24	0.31	0.17	0.22	1.2	0.49	1.1
400									
500									
630									

TABLE 4 (Continued)

4			5			6			7		
RACAL			RACAL			B & K			B & K		
14	18	15	14	18	15	14	18	15	14	18	15
Direction											
V	H	A	V	H	A	V	H	A	V	H	A
12	2.7	3.1	12	2.7	3.9	3.9	1.4	1.4	0.55	0.88	0.59
0.019	0.0039	0.0078	0.019	0.0078	0.0078	0.0039	0.0039	0.0039	0.00069	0.0014	0.00069
0.019	0.0039	0.0078	0.019	0.0078	0.0078	0.0039	0.0039	0.0039	0.00069	0.0022	0.0014
0.019	0.014	0.049	0.019	0.014	0.044	0.0039	0.017	0.049	0.00069	0.025	0.020
0.019	0.0087	0.039	0.019	0.0098	0.039	0.0039	0.0087	0.031	0.0012	0.012	0.014
0.019	0.0098	0.031	0.019	0.011	0.035	0.025	0.027	0.044	0.0044	0.015	0.020
0.15	0.14	0.14	0.14	0.15	0.15	0.055	0.077	0.22	0.0049	0.15	0.069
0.078	0.062	0.078	0.061	0.069	0.087	0.020	0.025	0.098	0.0028	0.055	0.031
0.055	0.078	0.055	0.039	0.069	0.035	0.039	0.035	0.055	0.0069	0.028	0.028
0.22	0.087	0.20	0.24	0.062	0.14	0.14	0.062	0.062	0.035	0.069	0.044
0.61	0.14	0.14	0.49	0.12	0.14	0.15	0.055	0.11	0.087	0.11	0.078
0.97	0.27	0.35	1.4	0.25	0.25	0.39	0.12	0.25	0.044	0.039	0.14
2.7	0.98	0.87	3.5	0.87	0.98	2.5	0.39	0.35	0.25	0.11	0.25
3.5	1.4	0.87	3.9	1.2	1.4	1.4	0.35	0.44	0.31	0.22	0.28
7.7	0.69	1.4	5.5	1.4	1.2	0.98	0.55	0.62	0.098	0.16	0.14
5.5	1.2	1.4	6.9	0.87	1.9	0.87	0.39	0.39	0.14	0.20	0.25
3.5	0.87	0.78	6.1	0.35	1.5	0.69	0.39	0.44	0.25	0.15	0.17
4.9	0.77	1.2	4.3	1.4	1.4	1.5	0.62	0.62	0.14	0.39	0.22
2.7	0.87	0.87	2.4	0.62	1.1	0.77	0.49	0.35	0.15	0.28	0.15
2.2	0.55	1.1	2.7	0.62	0.87	0.49	0.39	0.28	0.15	0.20	0.14
0.97	0.31	0.39	1.2	0.49	0.55	0.39	0.25	0.31	0.11	0.11	0.098
0.97	0.39	0.31	0.87	0.44	0.39	0.22	0.19	0.22	0.055	0.078	0.14
0.55	0.27	0.31	0.35	0.44	0.35	0.35	0.25	0.19	0.049	0.078	0.098
						0.27	0.27	0.17	0.049	0.49	0.078
						0.35	0.39	0.15	0.022	0.17	0.078
						0.19	0.25	0.14	0.035	0.049	0.062

TABLE 5

One-Third Octave Band RMS Acceleration Amplitudes on the Piles Supporting
Western Section of Powerhouse,
% Gravity, 90th Percentile

Pile Location	2			3			4			7		
Tape Recorder	RACAL			RACAL			RACAL			B & K		
Run No.	24	26	25	24	26	25	24	26	25	24	26	25
Frequency	Direction											
	V	H	A	V	H	A	V	H	A	V	H	A
Broadband	3.1	9.7	9.7	5.5	14	9.7	4.9	4.4	8.7	1.3	4.3	3.3
2.5	0.0087	0.031	0.019	0.019	0.022	0.017	0.0078	0.0098	0.019	0.0035	0.0049	0.0035
3.15	0.0078	0.024	0.019	0.019	0.019	0.017	0.0069	0.0087	0.019	0.0035	0.0049	0.0035
4.0	0.0078	0.019	0.044	0.019	0.022	0.039	0.0069	0.0069	0.043	0.0035	0.027	0.027
5.0	0.0078	0.019	0.031	0.019	0.019	0.027	0.0069	0.0069	0.031	0.0035	0.012	0.014
6.3	0.0098	0.019	0.027	0.019	0.019	0.022	0.0069	0.0078	0.019	0.022	0.025	0.025
8.0	0.15	0.087	0.31	0.14	0.15	0.17	0.028	0.11	0.11	0.015	0.15	0.087
10.0	0.087	0.044	0.14	0.061	0.077	0.087	0.014	0.055	0.055	0.0055	0.062	0.039
12.5	0.055	0.044	0.061	0.022	0.061	0.087	0.014	0.062	0.087	0.017	0.049	0.039
16	0.087	0.044	0.15	0.061	0.087	0.15	0.025	0.069	0.14	0.031	0.055	0.039
20	0.087	0.24	0.31	0.077	0.15	0.19	0.055	0.098	0.14	0.15	0.069	0.098
25	0.25	0.24	0.19	0.17	0.19	0.15	0.087	0.25	0.17	0.087	0.069	0.15
31.5	0.62	0.39	0.97	0.55	0.77	0.87	1.4	0.98	1.1	0.19	0.11	0.27
40	0.35	0.24	0.61	0.39	0.77	0.69	1.4	1.4	0.87	0.31	0.27	0.49
50	0.49	0.97	0.69	0.55	1.5	0.97	2.2	1.5	2.4	0.25	0.31	0.22
63	0.20	0.97	0.39	0.87	0.97	0.61	3.1	0.78	3.5	0.28	0.31	0.35
80	0.22	0.97	0.49	1.4	0.97	0.87	1.7	0.78	2.4	0.44	0.49	1.1
100	0.55	0.97	0.69	1.5	2.2	0.87	1.2	0.98	3.9	0.22	0.22	0.17
125	0.39	0.97	0.43	0.69	1.1	0.97	0.69	0.49	1.7	0.19	0.35	0.22
160	0.22	0.97	0.69	0.61	1.5	1.7	0.98	0.44	1.5	0.17	0.77	0.55
200	0.25	3.1	3.1	0.61	3.1	1.5	0.35	0.55	1.1	0.12	0.69	0.39
250	1.5	7.7	6.1	1.2	6.9	4.9	0.62	2.5	3.1	0.15	1.4	0.55
315	2.2	3.9	4.3	3.1	6.1	3.9	0.98	1.9	3.5	0.49	3.1	1.5
400	0.87	2.7	4.3	1.2	5.5	4.9	0.31	0.55	1.1	0.44	1.1	1.1
500	0.87	1.9	1.7	3.9	5.5	4.9	0.22	0.35	0.31	0.55	2.2	2.2
630	0.22	0.49	0.24	1.5	2.4	1.2	0.12	0.15	0.19	0.25	0.69	0.62

TABLE 6

One-Third Octave Band RMS Acceleration Amplitudes
on the Floor of the Eastern Section of the Powerhouse,
% Gravity, 90th Percentile

Floor Location*	1			2			3		
Tape Recorder	RACAL			RACAL			RACAL		
Run No.	7	11	10	7	11	10	7	11	10
	Direction								
Frequency	V	H	A	V	H	A	V	H	A
Broadband	0.27	0.35	0.55	0.31	0.69	0.39	0.49	0.55	0.31
2.5	0.00039	0.00078	0.00078	0.00039	0.00078	0.00078	0.00078	0.00078	0.00078
3.15	0.00039	0.0014	0.00078	0.00039	0.00078	0.00078	0.00078	0.00087	0.00078
4.0	0.0011	0.015	0.0031	0.00044	0.0017	0.0035	0.00078	0.0069	0.0062
5.0	0.00080	0.0098	0.0025	0.00039	0.0020	0.0022	0.00078	0.0044	0.0044
6.3	0.00062	0.012	0.0078	0.00049	0.0062	0.0062	0.00078	0.0078	0.0087
8.0	0.0055	0.098	0.15	0.0044	0.098	0.11	0.0014	0.11	0.14
10.0	0.0025	0.049	0.069	0.0022	0.044	0.049	0.00098	0.049	0.062
12.5	0.0055	0.039	0.035	0.0015	0.049	0.022	0.0012	0.028	0.035
16	0.0077	0.098	0.028	0.0078	0.11	0.011	0.0069	0.035	0.078
20	0.020	0.062	0.055	0.0070	0.087	0.031	0.012	0.044	0.055
25	0.044	0.049	0.17	0.028	0.078	0.049	0.044	0.078	0.044
31.5	0.078	0.19	0.25	0.14	0.39	0.19	0.20	0.31	0.15
40	0.15	0.087	0.39	0.14	0.44	0.25	0.31	0.39	0.12
50	0.15	0.15	0.15	0.15	0.19	0.17	0.17	0.15	0.087
63	0.098	0.11	0.098	0.12	0.087	0.087	0.22	0.14	0.11
80	0.049	0.078	0.069	0.049	0.087	0.035	0.17	0.069	0.087
100	0.069	0.039	0.035	0.077	0.12	0.039	0.062	0.055	0.055
125	0.049	0.055	0.020	0.035	0.098	0.028	0.044	0.044	0.039
160	0.069	0.069	0.022	0.035	0.055	0.028	0.044	0.055	0.035
200	0.055	0.039	0.017	0.027	0.028	0.022	0.039	0.031	0.031
250	0.039	0.031	0.015	0.027	0.022	0.015	0.028	0.025	0.031
315	0.027	0.020	0.012	0.019	0.017	0.014	0.022	0.015	0.022
400									
500									
630									

*Measurements were not taken at location 6 because of time constraints

TABLE 6 (Continued)

4			5			7			8		
RACAL			RACAL			B & K			B & K		
7	11	10	7	11	10	7	11	10	7	11	10
Direction											
V	H	A	V	H	A	V	H	A	V	H	A
0.49	0.49	0.35	0.62	0.78	0.49	0.87	0.55	0.78	3.5	1.2	1.6
0.00078	0.00078	0.00078	0.00078	0.0016	0.00078	0.00078	0.00078	0.0015	0.0035	0.0035	0.0039
0.00078	0.00078	0.00078	0.00078	0.0016	0.00098	0.00078	0.0014	0.0028	0.0035	0.0035	0.0039
0.00078	0.0020	0.0049	0.00078	0.0069	0.014	0.0022	0.015	0.039	0.0035	0.0078	0.039
0.00078	0.0020	0.0035	0.00078	0.0049	0.0087	0.0015	0.0078	0.020	0.0035	0.0044	0.017
0.00078	0.0062	0.0069	0.00078	0.0087	0.0098	0.0055	0.012	0.020	0.019	0.025	0.031
0.0069	0.098	0.12	0.0049	0.11	0.11	0.022	0.078	0.15	0.0098	0.098	0.11
0.0031	0.044	0.055	0.0022	0.049	0.055	0.0078	0.028	0.062	0.0049	0.039	0.044
0.0025	0.049	0.031	0.0020	0.028	0.055	0.0049	0.035	0.069	0.017	0.062	0.049
0.0035	0.11	0.078	0.012	0.020	0.069	0.015	0.055	0.22	0.022	0.078	0.12
0.0069	0.078	0.049	0.028	0.049	0.044	0.055	0.028	0.17	0.039	0.098	0.098
0.039	0.069	0.049	0.044	0.078	0.11	0.055	0.062	0.14	0.14	0.15	0.15
0.15	0.31	0.15	0.14	0.35	0.28	0.17	0.12	0.20	0.44	0.35	0.49
0.31	0.28	0.17	0.31	0.49	0.14	0.22	0.31	0.31	1.7	0.69	0.39
0.17	0.20	0.15	0.17	0.25	0.15	0.31	0.25	0.20	2.2	0.19	0.69
0.28	0.12	0.098	0.12	0.31	0.17	0.39	0.11	0.28	1.4	0.44	0.69
0.12	0.078	0.078	0.35	0.22	0.22	0.35	0.15	0.11	1.7	0.49	0.77
0.087	0.069	0.020	0.20	0.25	0.087	0.35	0.25	0.11	0.98	0.49	0.49
0.055	0.069	0.022	0.25	0.14	0.087	0.31	0.11	0.062	0.39	0.55	0.39
0.031	0.035	0.025	0.12	0.062	0.078	0.25	0.087	0.062	0.27	0.27	0.27
0.035	0.022	0.015	0.055	0.035	0.049	0.17	0.078	0.078	0.22	0.098	0.17
0.025	0.020	0.015	0.055	0.035	0.031	0.11	0.069	0.055	0.11	0.087	0.077
0.020	0.014	0.012	0.049	0.039	0.039	0.17	0.069	0.31	0.12	0.098	0.077
						0.17	0.098	0.31	0.0087	0.098	0.098
						0.055	0.062	0.049	0.0049	0.055	0.055
						0.069	0.098	0.078	0.0039	0.049	0.044

TABLE 7

One-Third Octave Band RMS Acceleration Amplitudes on the Piles Supporting Eastern Section of the Powerhouse, % Gravity, 90th Percentile

Pile Location	1			2			3		
Tape Recorder	RACAL			RACAL			RACAL		
Run No.	20	22	23	20	22	23	20	22	23
				Direction					
Frequency	V	H	A	V	H	A	V	H	A
Broadband	0.27	0.49	0.55	0.27	0.78	0.49	0.44	0.49	0.44
2.5	0.00049	0.00078	0.00087	0.00062	0.00098	0.0012	0.00087	0.00069	0.00078
3.15	0.00039	0.0014	0.00098	0.00055	0.00098	0.0011	0.00078	0.00087	0.00078
4.0	0.0015	0.014	0.0017	0.00049	0.0012	0.0028	0.00078	0.0049	0.0055
5.0	0.00087	0.0098	0.0025	0.00044	0.0015	0.0025	0.00078	0.0035	0.0049
6.3	0.00049	0.012	0.0098	0.00044	0.0055	0.0069	0.00078	0.0078	0.0087
8.0	0.0049	0.087	0.17	0.0025	0.087	0.12	0.0031	0.098	0.12
10.0	0.0025	0.044	0.078	0.0014	0.039	0.055	0.0015	0.049	0.055
12.5	0.0039	0.025	0.031	0.0039	0.039	0.017	0.0015	0.022	0.025
16	0.0055	0.087	0.031	0.0062	0.098	0.014	0.0062	0.022	0.078
20	0.020	0.055	0.078	0.0049	0.062	0.031	0.012	0.044	0.049
25	0.062	0.035	0.15	0.035	0.11	0.044	0.098	0.087	0.078
31.5	0.12	0.12	0.19	0.12	0.44	0.22	0.31	0.35	0.28
40	0.11	0.14	0.35	0.14	0.49	0.31	0.11	0.22	0.078
50	0.15	0.14	0.15	0.14	0.35	0.22	0.11	0.17	0.11
63	0.11	0.19	0.11	0.098	0.17	0.087	0.17	0.12	0.14
80	0.069	0.17	0.098	0.049	0.14	0.035	0.14	0.098	0.078
100	0.049	0.098	0.062	0.087	0.15	0.049	0.055	0.049	0.049
125	0.055	0.087	0.025	0.049	0.069	0.035	0.055	0.055	0.039
160	0.062	0.12	0.022	0.049	0.098	0.049	0.055	0.069	0.049
200	0.039	0.078	0.028	0.035	0.062	0.028	0.044	0.049	0.031
250	0.035	0.069	0.028	0.031	0.044	0.022	0.062	0.15	0.028
315	0.025	0.069	0.035	0.022	0.031	0.035	0.087	0.069	0.049
400	0.035	0.22	0.15	0.027	0.039	0.069	0.031	0.028	0.087
500	0.055	0.062	0.087	0.035	0.039	0.11	0.028	0.020	0.15
630	0.039	0.078	0.098	0.039	0.062	0.055	0.022	0.012	0.055

TABLE 7 (Continued)

4			5			6			7		
RACAL			RACAL			RACAL			B & K		
20	22	23	20	22	23	20	22	23	20	22	23
Direction											
V	H	A	V	H	A	V	H	A	V	H	A
0.44	0.49	0.39	0.44	0.97	0.69	0.69	1.7	1.1	0.97	2.4	1.5
0.0012	0.00087	0.0011	0.00087	0.0019	0.0022	0.0027	0.0044	0.0024	0.00098	0.0039	0.0039
0.0011	0.00078	0.00098	0.00078	0.0019	0.0022	0.0022	0.0039	0.0024	0.0011	0.0039	0.0039
0.00078	0.0011	0.0049	0.00078	0.0035	0.014	0.0017	0.0069	0.015	0.0035	0.0098	0.039
0.00078	0.0015	0.0044	0.00078	0.0031	0.012	0.0017	0.0049	0.014	0.0022	0.0062	0.025
0.00078	0.0055	0.0087	0.00078	0.0077	0.015	0.0017	0.0078	0.015	0.0049	0.025	0.035
0.0035	0.087	0.12	0.00098	0.097	0.12	0.0044	0.078	0.12	0.020	0.077	0.15
0.0020	0.039	0.055	0.00087	0.044	0.055	0.0024	0.039	0.055	0.0069	0.027	0.055
0.0062	0.039	0.022	0.0031	0.027	0.043	0.0035	0.025	0.043	0.0044	0.027	0.055
0.011	0.098	0.062	0.0069	0.024	0.061	0.019	0.087	0.049	0.0062	0.069	0.19
0.0098	0.069	0.044	0.012	0.061	0.049	0.022	0.062	0.097	0.044	0.039	0.15
0.062	0.069	0.039	0.020	0.12	0.097	0.035	0.035	0.11	0.069	0.044	0.15
0.19	0.28	0.14	0.078	0.43	0.17	0.12	0.098	0.17	0.12	0.14	0.17
0.25	0.28	0.12	0.22	0.49	0.15	0.097	0.14	0.097	0.15	0.31	0.31
0.12	0.069	0.17	0.14	0.27	0.15	0.22	0.25	0.24	0.28	0.22	0.17
0.19	0.049	0.098	0.087	0.24	0.19	0.15	0.15	0.077	0.35	0.25	0.17
0.11	0.078	0.055	0.25	0.27	0.15	0.17	0.15	0.15	0.31	0.35	0.25
0.069	0.069	0.055	0.14	0.19	0.12	0.17	0.22	0.15	0.39	0.35	0.55
0.044	0.062	0.031	0.17	0.14	0.11	0.14	0.12	0.19	0.22	0.31	0.11
0.049	0.049	0.044	0.12	0.17	0.15	0.087	0.17	0.31	0.15	0.35	0.11
0.031	0.035	0.035	0.069	0.077	0.15	0.14	0.77	0.49	0.15	0.35	0.12
0.025	0.044	0.062	0.044	0.049	0.061	0.12	0.49	0.77	0.098	0.35	0.098
0.031	0.087	0.098	0.049	0.22	0.19	0.27	0.77	0.19	0.22	1.5	0.49
0.035	0.069	0.14	0.098	0.31	0.43	0.39	1.2	0.27	0.44	1.5	0.98
0.049	0.098	0.031	0.049	0.097	0.087	0.055	0.12	0.15	0.20	0.15	0.39
0.022	0.025	0.025	0.025	0.039	0.014	0.043	0.055	0.055	0.28	0.14	0.55

TABLE 8

Broadband RMS Acceleration Amplitudes in Eastern Section of Powerhouse, % Gravity, 90th Percentile

Location		Minimum Distance To Generator Cradle (m)	Broadband RMS Amplitudes* % Gravity		
Number	Structure		Vertical	Horizontal	Axial
1	Floor	24.4	0.27	0.35	0.55
	Pile		0.26	0.42	0.51
2	Floor	24.0	0.31	0.69	0.39
	Pile		0.27	0.77	0.47
3	Floor	16.6	0.49	0.55	0.31
	Pile		0.43	0.49	0.40
4	Floor	16.6	0.49	0.49	0.35
	Pile		0.43	0.47	0.36
5	Floor	9.1	0.62	0.78	0.49
	Pile		0.42	0.91	0.53
6	Floor	8.0	-	-	-
	Pile		0.56	1.2	1.0
7	Floor	4.6	0.85	0.52	0.71
	Pile		0.81	1.9	0.98
8	Floor	3.4	3.5	1.2	1.5
	Pile		-	-	-

*Bandwidth 0-315 Hz.

TABLE 9

One-Third Octave Band RMS Acceleration Amplitudes on the Freestanding Pile, % Gravity, 90th Percentile

Location	Free Pile		
	B & K		
Tape Recorder Run No.	24	26	25
Frequency	Direction Vertical	Horizontal	Axial
Broadband	0.17	0.27	0.27
2.5	0.0068	0.027	0.014
3.15	0.0076	0.027	0.015
4.0	0.0061	0.030	0.014
5.0	0.0061	0.034	0.014
6.3	0.024	0.038	0.019
8.0	0.012	0.030	0.015
10.0	0.0068	0.027	0.0096
12.5	0.024	0.030	0.030
16	0.022	0.024	0.054
20	0.038	0.054	0.054
25	0.054	0.086	0.068
31.5	0.043	0.076	0.086
40	0.034	0.086	0.086
50	0.034	0.11	0.14
63	0.038	0.12	0.11
80	0.043	0.096	0.12
100	0.038	0.054	0.043
125	0.076	0.061	0.061
160	0.043	0.043	0.043
200	0.034	0.034	0.034
250	0.043	0.043	0.038
315	0.048	0.048	0.043
400	0.038	0.038	0.034
500	0.027	0.027	0.024
630	0.015	0.011	0.014

TABLE 10

Broadband RMS Acceleration Amplitudes on Piles at Powerhouse, % Gravity, 90th Percentile

Location	Distance From Freestanding Pile (m)	Minimum Distance From a Cradle Pile (m)	Broadband RMS Amplitudes (% Gravity)		
			Vertical	Horizontal	Axial
Freestanding Pile	0	11.1	0.17	0.27	0.27
Minimum Pile Amplitude at Powerhouse					
Pile 1 Eastern Section	17.1	24.4	0.27	0.49	
Pile 4 Eastern Section	21.6	16.7		0.49	0.39
Pile in Each Structurally Isolated System of Powerhouse Nearest to Freestanding Pile					
Pile 7 Eastern Section	6.2	5.2	0.97	2.4	1.5
Pile 2 Western Section	8.2	6.5	3.1	9.7	9.7
Pile 5 Cradle	11.1	0	22	69	55

TABLE 11

One-Third Octave Band RMS Acceleration Amplitudes in Powerhouse With Generator Turned Off, % Gravity, 90th Percentile

	Generator	Generator Cradle	Piles Under Generator Cradle			Piles Under Western Section		Piles Under Eastern Section	
Location	13	2	5	5	6	4	7	1	2
Tape Recorder Run No.	RACAL 30	RACAL 30	RACAL 30	RACAL 30	RACAL 30	RACAL 30	RACAL 30	B & K 30	B & K 30
			Direction						
Frequency	H	H	V	A	H	H	A	H	A
Broadband	0.83	0.25	0.077	0.11	0.086	0.25	0.69	0.11	0.062
2.5	0.10	0.00035	0.00017	0.00035	0.00035	0.00039	0.0019	0.00039	0.00035
3.15	0.093	0.00087	0.00017	0.00035	0.00062	0.00049	0.0019	0.00087	0.00049
4.0	0.093	0.0014	0.00017	0.00055	0.0011	0.00062	0.0019	0.0014	0.00049
5.0	0.083	0.0019	0.00039	0.0019	0.0035	0.00087	0.0027	0.0012	0.00069
6.3	0.074	0.0011	0.00049	0.0027	0.0035	0.0012	0.0024	0.0039	0.0025
8.0	0.059	0.00087	0.00039	0.0017	0.0014	0.0015	0.0031	0.0027	0.0022
10.0	0.052	0.0017	0.00077	0.0025	0.0035	0.0039	0.0069	0.0035	0.0035
12.5	0.037	0.0044	0.0012	0.0044	0.0087	0.0078	0.0087	0.0044	0.0049
16	0.029	0.0069	0.0027	0.0027	0.0069	0.0028	0.0061	0.0044	0.0035
20	0.021	0.022	0.0087	0.0062	0.0031	0.0055	0.0024	0.0077	0.0039
25	0.042	0.035	0.0069	0.0062	0.0087	0.022	0.069	0.017	0.0069
31.5	0.13	0.12	0.024	0.019	0.027	0.087	0.31	0.055	0.022
40	0.010	0.022	0.0049	0.0035	0.0039	0.019	0.043	0.0069	0.0098
50	0.026	0.055	0.012	0.0069	0.0098	0.027	0.055	0.014	0.0069
63	0.066	0.098	0.049	0.017	0.027	0.098	0.097	0.031	0.019
80	0.021	0.087	0.027	0.015	0.019	0.044	0.39	0.027	0.017
100	0.029	0.11	0.024	0.017	0.017	0.098	0.087	0.0098	0.0069
125	0.023	0.078	0.031	0.022	0.019	0.062	0.069	0.014	0.0062
160	0.026	0.039	0.035	0.022	0.039	0.069	0.14	0.022	0.0055
200	0.017	0.031	0.014	0.027	0.027	0.12	0.087	0.014	0.0069
250	0.0093	0.025	0.012	0.055	0.014	0.062	0.17	0.017	0.022
315	0.0083	0.025	0.011	0.055	0.025	0.055	0.27	0.019	0.027
400	0.0074	0.031	0.0055	0.055	0.049	0.035	0.19	0.069	0.039
500	0.0042	0.017	0.0031	0.012	0.025	0.025	0.27	0.012	0.0055
630	0.0029	0.0098	0.0044	0.0019	0.014	0.022	0.087	0.0049	0.0049
Broadband RMS Acceleration Amplitudes With Generator On									
	23.0	18.0*	22.0	55.0	44.0	4.4	3.3	0.49	0.49

*0-315 Hz

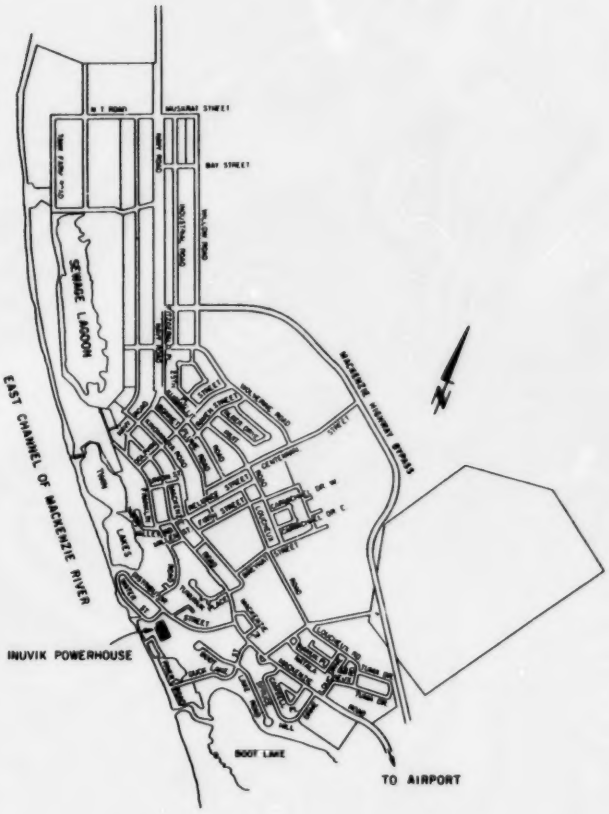

Figure 1. Inuvik, N.W.T.

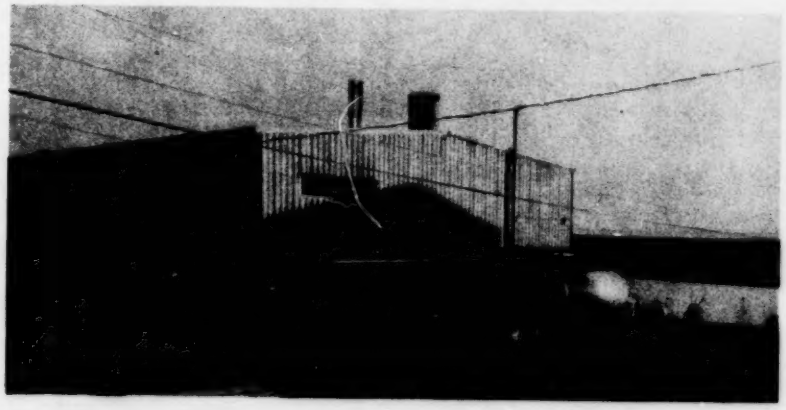

Figure 2. West side of Inuvik powerhouse. East channel of Mackenzie River on right.

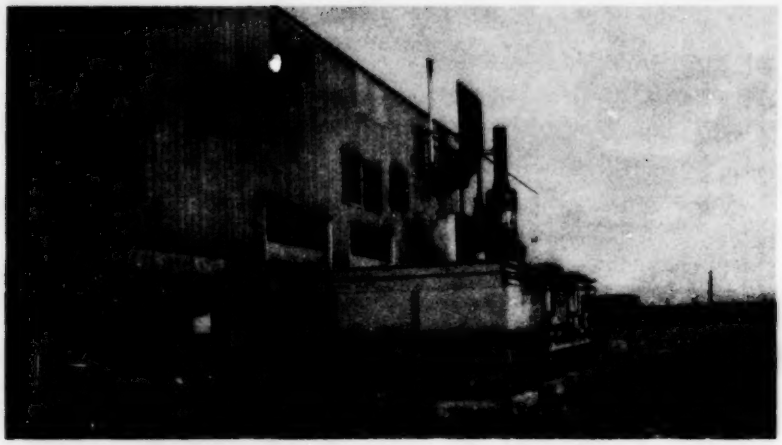

Figure 3. South (river) side of Inuvik powerhouse.

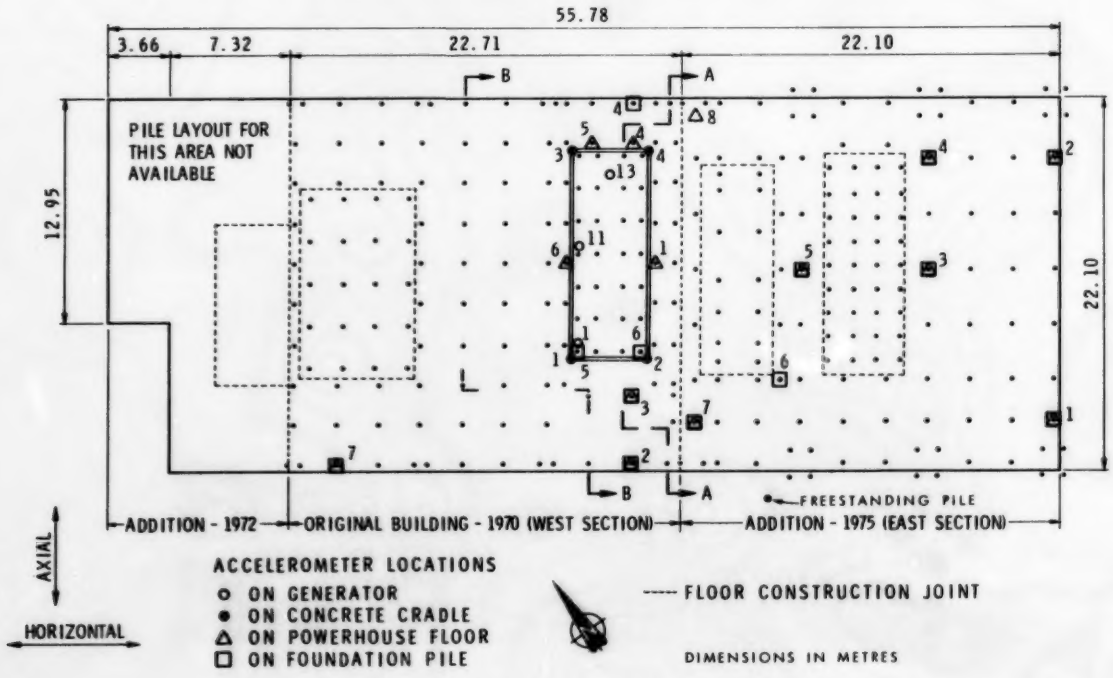

Figure 4. Northern Canada Power Commission powerhouse, Inuvik, N.W.T. (Sections A-A and B-B shown in figures 6 and 8.)

Figure 5. Ground surface at east end of Inuvik powerhouse.

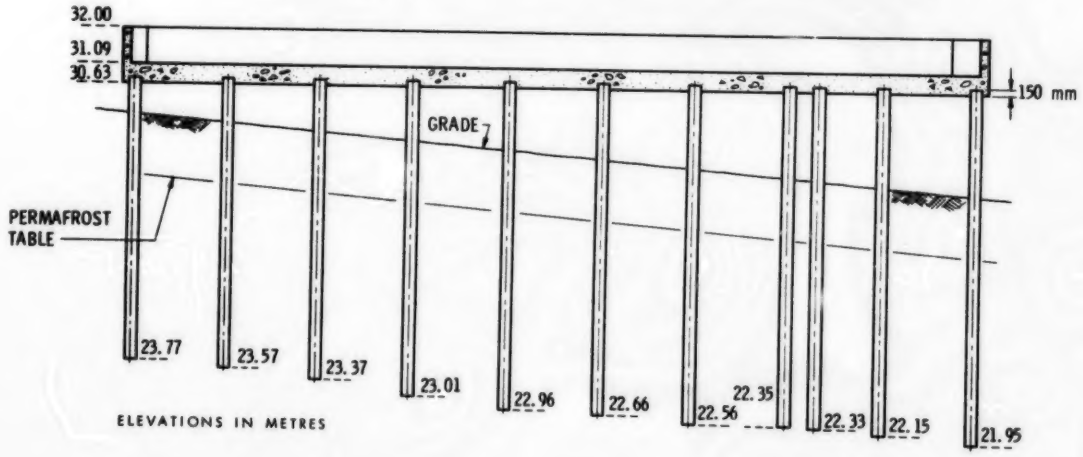

Figure 6. Section B-B (from figure 4) through western section of powerhouse.

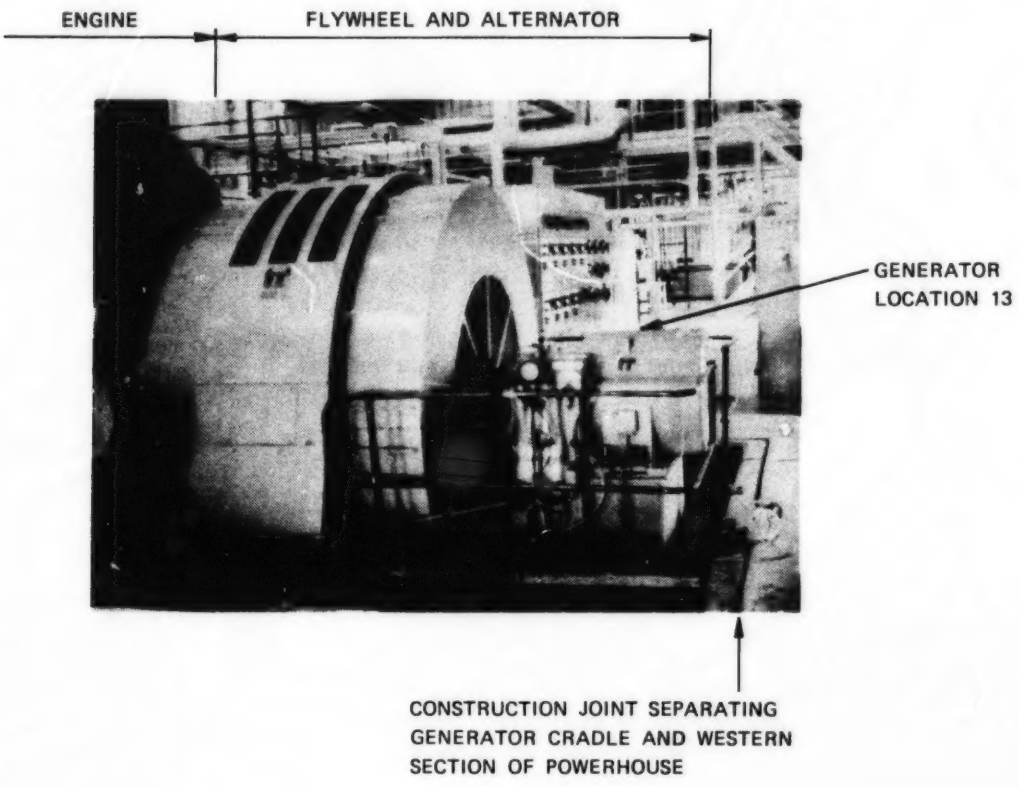

Figure 7. Flywheel and alternator of main diesel generator.

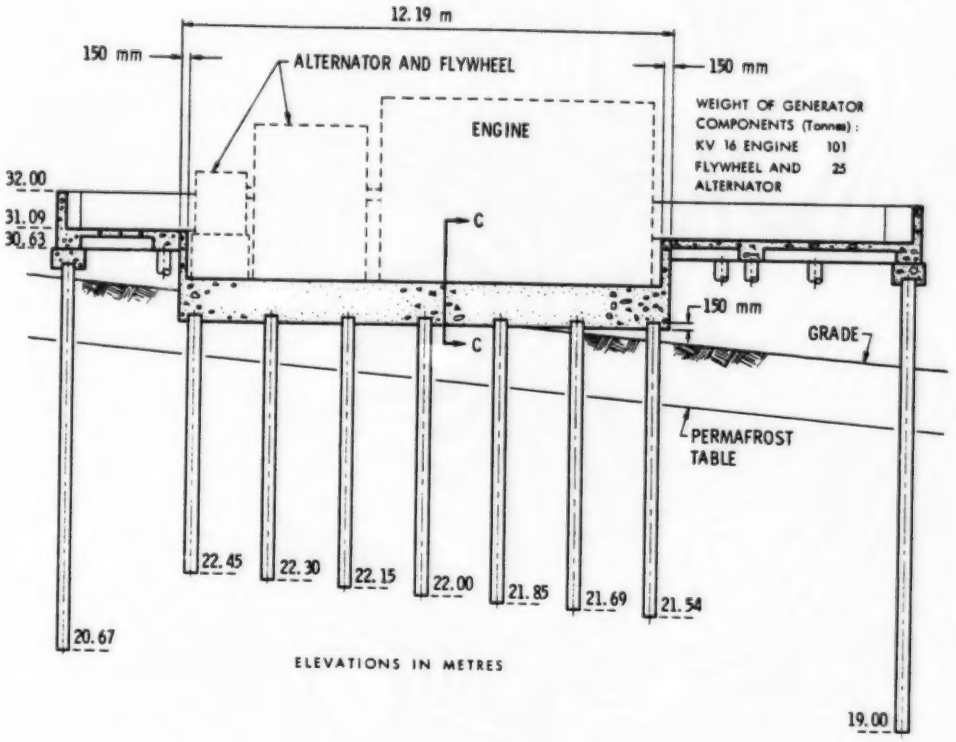

Figure 8. Section A-A (from figure 4) through main diesel generator. (Section C-C shown in figure 9.)

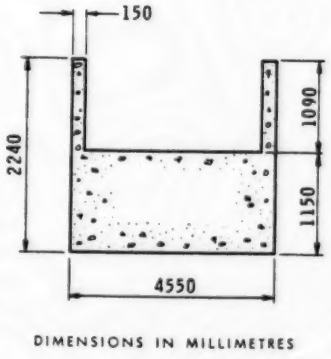

Figure 9. Section C-C (from figure 8) through cradle of main diesel generator.

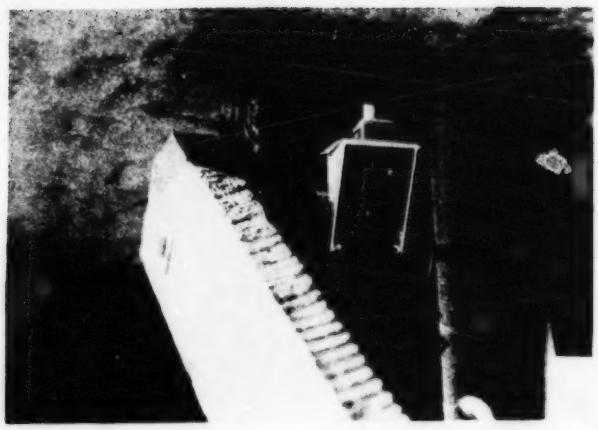

Figure 10. Aluminum frame for securing Q-flex accelerometers to wood piles.

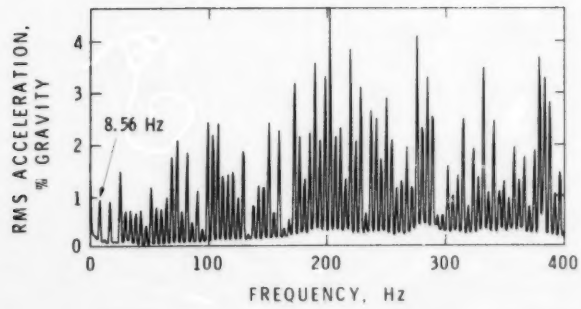

Figure 11. Frequency spectrum, vertical direction, generator location 1.

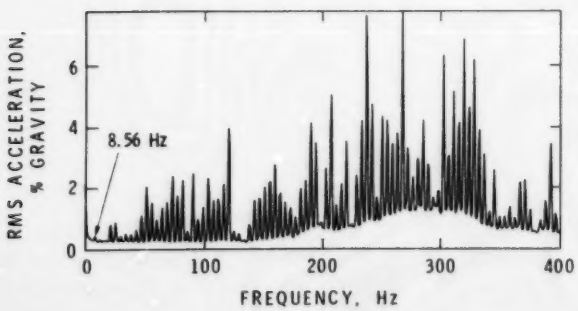

Figure 12. Frequency spectrum, vertical direction, generator location 11.

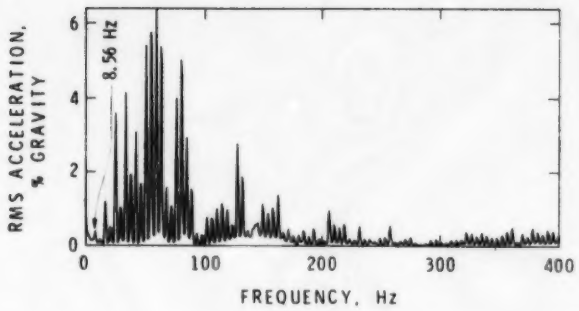

Figure 13. Frequency spectrum, vertical direction, generator location 13.

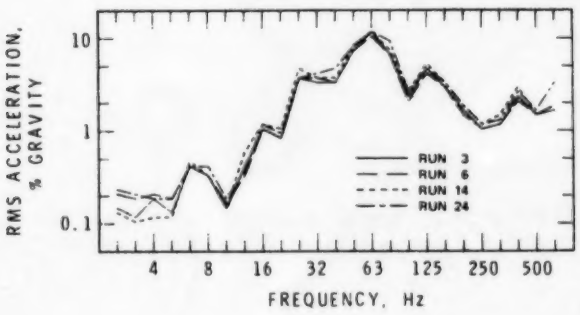

Figure 14. One-third octave band spectra, vertical direction, generator location 13.

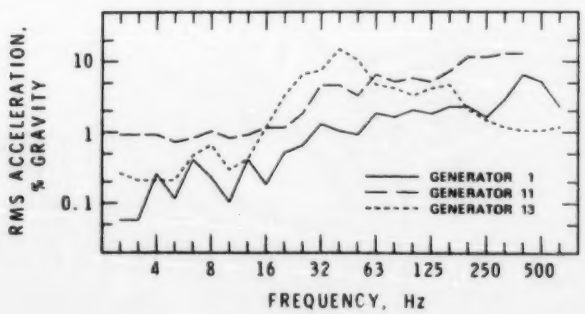

Figure 15. One-third octave band spectra, horizontal direction, generator.

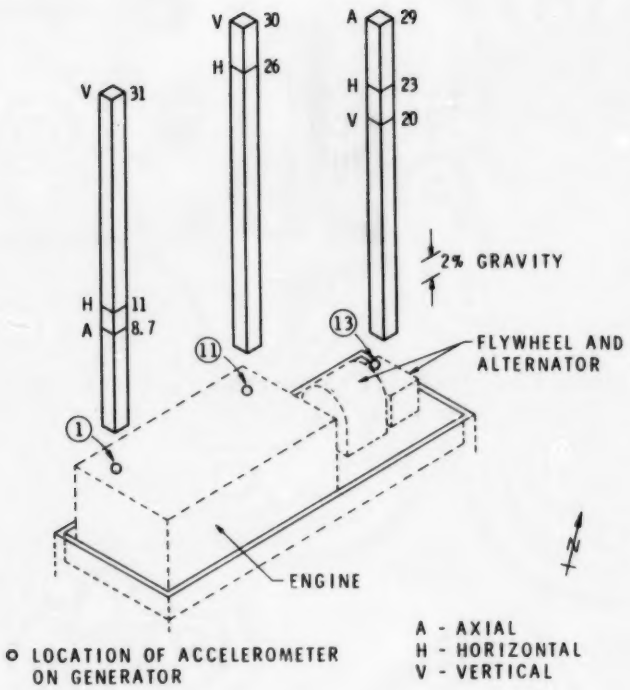

Figure 16. Broadband RMS acceleration amplitudes (percent gravity) on generator.

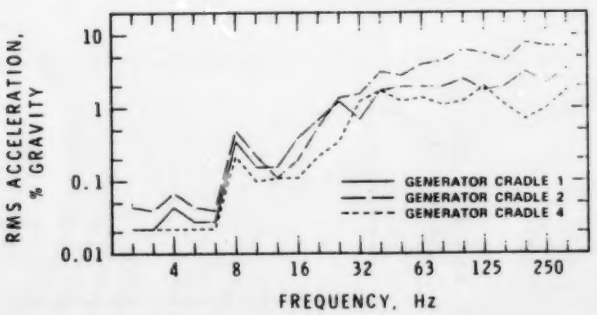

Figure 17. One-third octave band spectra, horizontal direction, generator cradle.

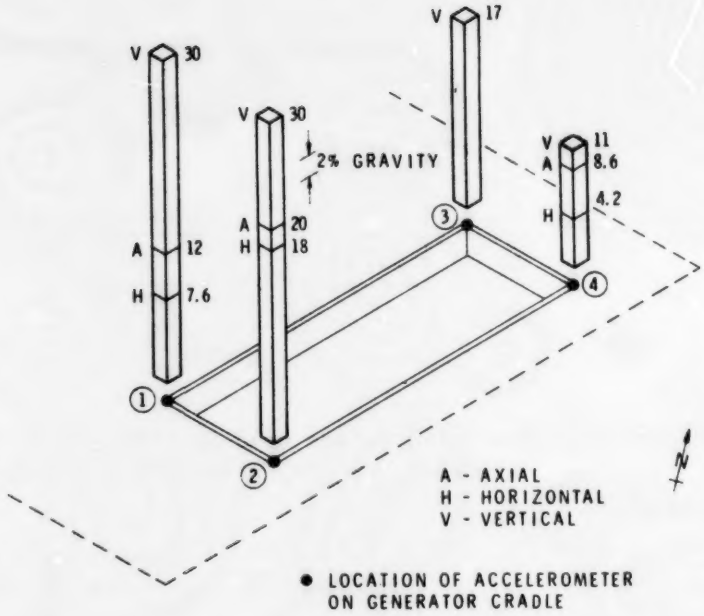

Figure 18. Broadband RMS acceleration amplitudes (percent gravity) on generator cradle.

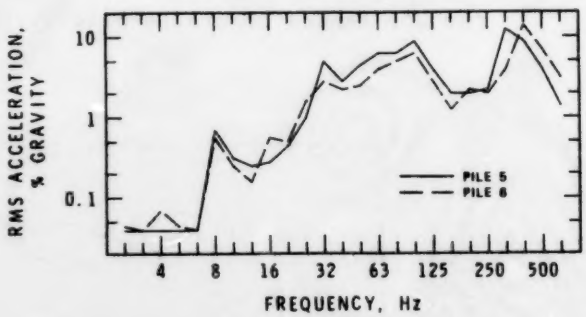

Figure 19. One-third octave band spectra, vertical direction, piles supporting generator cradle.

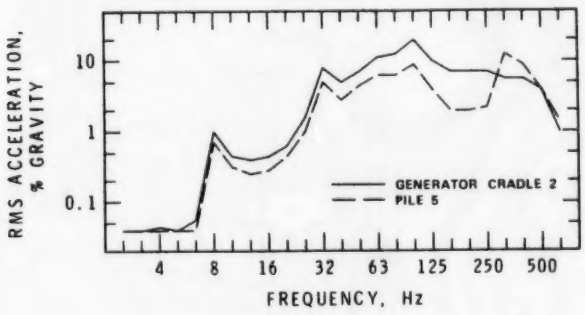

Figure 20. One-third octave band spectra, vertical direction, run 24, generator cradle-pile system.

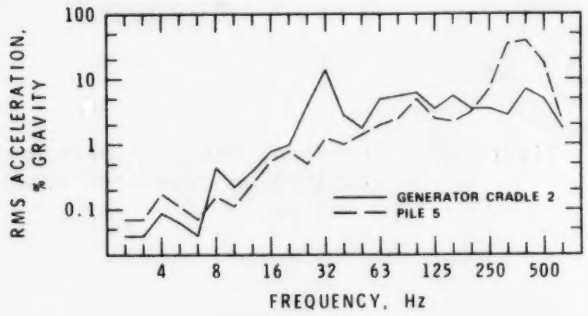

Figure 21. One-third octave band spectra, axial direction, run 25, generator cradle-pile system.

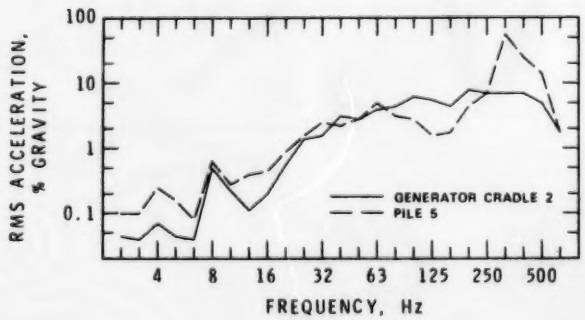

Figure 22. One-third octave band spectra, horizontal direction, run 26, generator cradle-pile system.

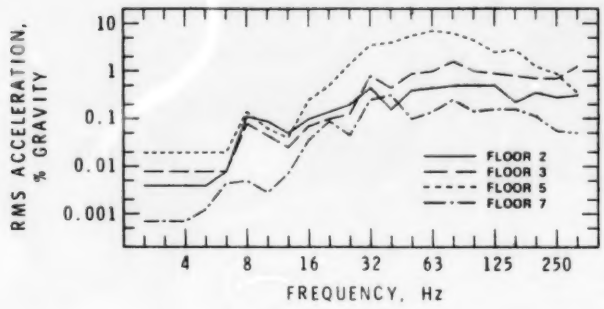

Figure 23. One-third octave band spectra, vertical direction, floor of western section of powerhouse.

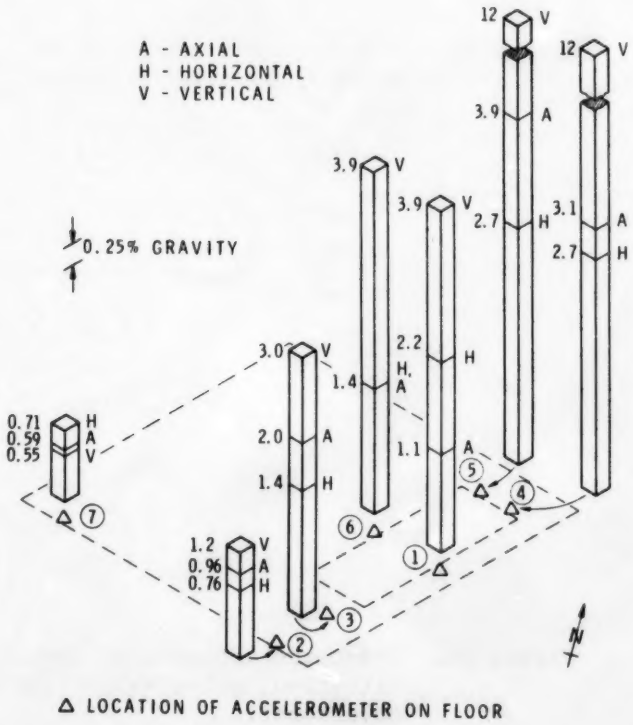

Figure 24. Broadband (0-315 Hz) RMS acceleration amplitudes (percent gravity) on floor of western section of powerhouse.

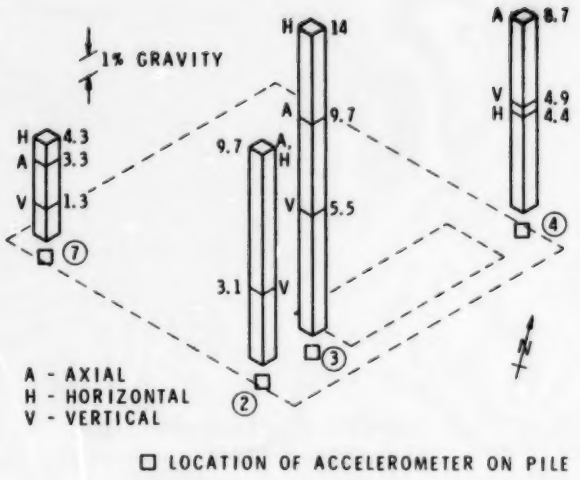

Figure 25. Broadband RMS acceleration amplitudes (percent gravity) on piles supporting western section of powerhouse.

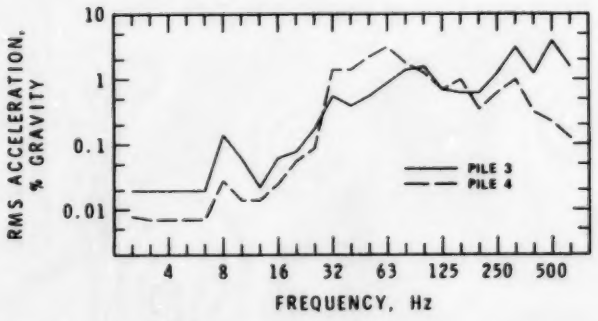

Figure 26. One-third octave band spectra, vertical direction, piles supporting western section of powerhouse.

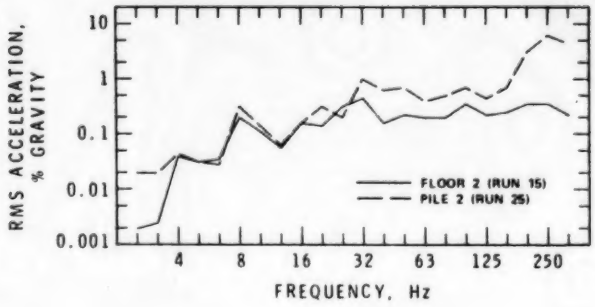

Figure 27. One-third octave band spectra, axial direction, floor and pile of western section of powerhouse.

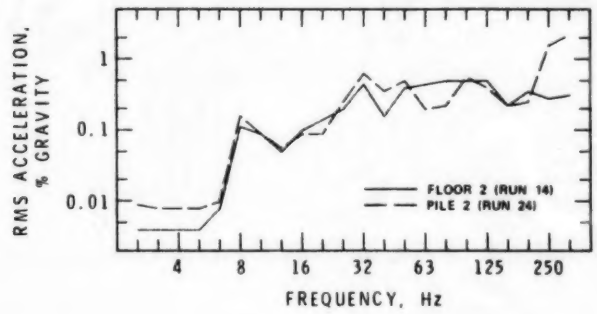

Figure 28. One-third octave band spectra, vertical direction, floor and pile of western section of powerhouse.

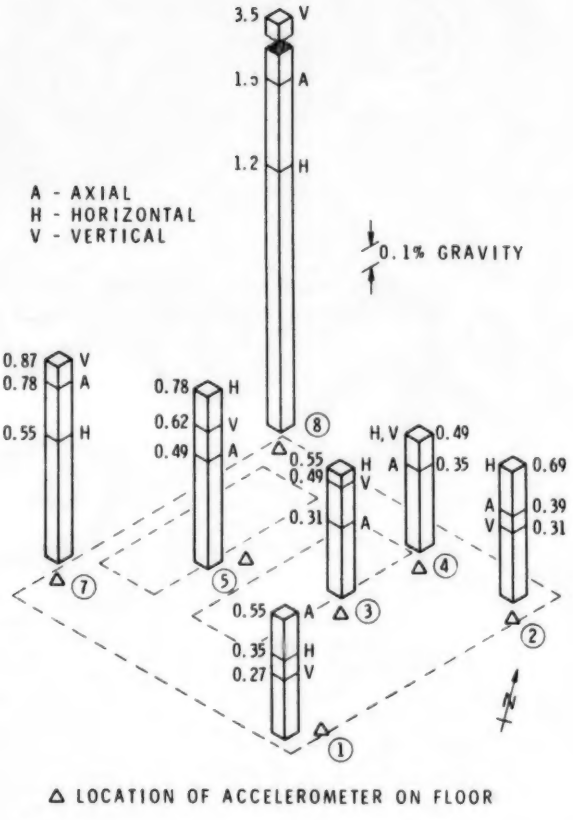

Figure 29. Broadband RMS acceleration amplitudes (percent gravity) on floor of eastern section of powerhouse.

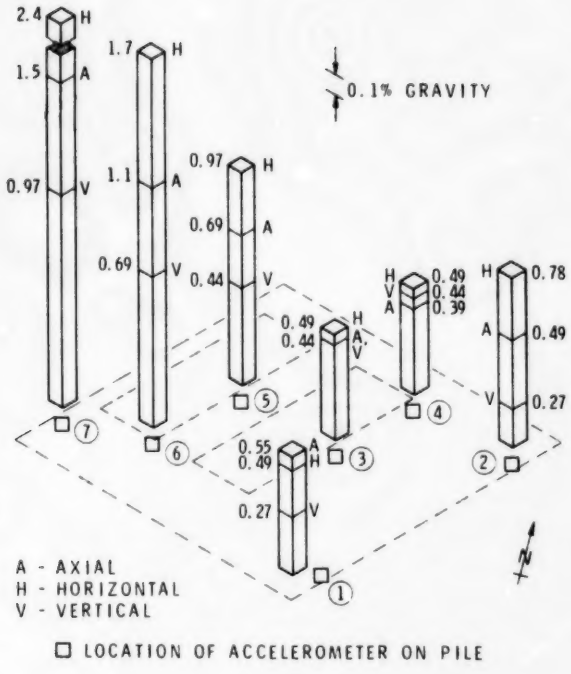

Figure 30. Broadband RMS acceleration amplitudes (percent gravity) on piles supporting eastern section of powerhouse.

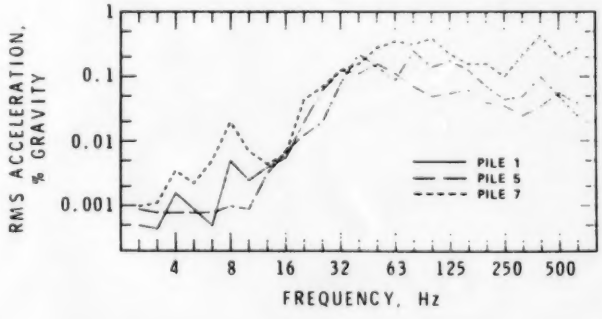

Figure 31. One-third octave band spectra, vertical direction, piles supporting eastern section of powerhouse.

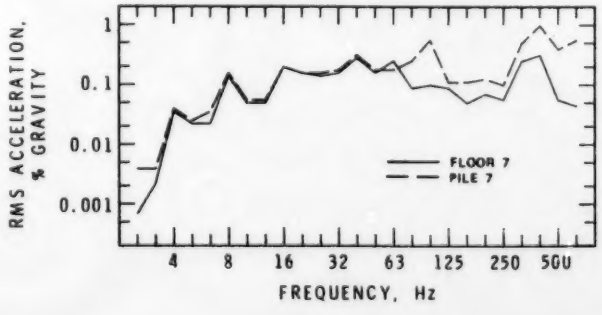

Figure 32. One-third octave band spectra, axial direction, run 23, floor and pile of eastern section of powerhouse.